Microstructure/Mechanical Property Relationships in Thick-Section C-Mn Narrow-Groove Welds

With a careful control of welding wire chemistry and flux basicity, optimum strength and toughness were achieved in pressure vessel steel

BY J. T. McGRATH, R. S. CHANDEL, R. F. ORR AND J. A. GIANETTO

ABSTRACT. The mechanical properties of a series of submerged arc, narrow-groove welds deposited in thick-section SA516 Gr. 70 pressure vessel steel were evaluated in terms of chemical composition and microstructure. The weld chemistry was controlled by the selection of welding wire and flux basicity.

Optimum strength and low-temperature notch toughness were achieved in weld metals containing a high proportion of acicular ferrite in the as-deposited columnar region and fine polygonal ferrite in the reheated region.

It was found that excessive amounts of oxygen (≥0.08%) and molybdenum (0.5%) promoted the formation of coarse-grain boundary ferrite and ferrite with second phase, which were detrimental to low-temperature notch toughness properties. In addition, high silicon (0.8%) was also found to have a deleterious effect on toughness.

Improved resistance to ductile fracture, *i.e.*, highest upper shelf Charpy energy was associated with a low-inclusion content (O + S < 0.030%).

The evaluation of the effect of notch position on weld metal notch toughness by placing the notch at the ¼-width and the ½-width positions in the two-pass per layer welds was inconclusive.

Introduction

The interest in narrow-groove welding of thick-section pressure vessel steels has focused primarily on Cr-Mo steels for applications such as reactor vessels for the hydrotreatment of heavy oils or tar sands bitumen (Refs. 1, 2). In the 2.25Cr-1Mo weld deposits, optimization of weld-metal microstructure and mechanical properties indicated that a fine, bainitic structure combined with low-inclusion content (O + S < 0.035%) resulted in high notch toughness properties. Furthermore, it was found that for two-pass per layer submerged arc narrow-groove welds there was little difference in notch toughness in welds notched in the region containing predominantly the as-deposited microstructure (¼-width position) compared with specimens notched at the ½-width position, which contained mainly reheated structure.

The current program was undertaken to investigate factors controlling the microstructure/mechanical property relationships in narrow-groove welds prepared in a more conventional thick-section SA516 Gr. 70 C-Mn pressure vessel steel. The microstructure of multi-pass C-Mn welds is more complicated than the Cr-Mo welds in that the as-deposited and reheated regions contain a variety of microstructural constituents that can affect mechanical properties.

J. T. McGRATH, R. S. CHANDEL, R. F. ORR and J. A. GIANETTO are with the Welding Section, Canada Centre for Mineral and Energy Technology, Ottawa, Canada.

KEY WORDS

Submerged Arc
Narrow-Groove Welds
Thick-Section Welds
C-Mn Steel Welds
SA516 GR 70 Steel
C-Mn Microstructure
Low-Temp. Toughness
Notch Toughness
Wire-Flux Basicity
Excessive Oxygen

Experimental

Weld Preparation

Experimental welds were deposited in a 76-mm (3-in.) thick SA516 Gr. 70 steel (Table 1) using an AC square-wave submerged arc, narrow-groove process.

A joint design consisting of an 8-deg included angle and a 16-mm (0.63-in.) root opening was used for the experimental welds, as shown in Fig. 1. The primary objective in selecting the welding wires and fluxes was to produce a weld composition and microstructure that would achieve the targeted tensile properties of 275-MPa (40-ksi) yield strength and 482-MPa (70-ksi) ultimate tensile strength, and a notch toughness of 27 J (20 ft-lb) at −40°C (−40°F) after post-weld heat treatment. The optimization of weld microstructure was through control of the weld metal chemistry (hardenability) and inclusion content.

The consumables chosen for the program are listed in Table 2. The principal source of hardenability in Welds NG-1 and NG-2 comes from additions of carbon (0.1%) and manganese (1.2–1.9%) in the welding wire. The high level of silicon in the wire for Weld NG-2 acts as a deoxident. In Welds NG-3 and NG-4, molybdenum contributes to hardenability, along with carbon and manganese. The control of inclusions in the weld metals was based on the selection of fluxes with basicities ranging from 1.0 to 3.0—Table 2.

Bead-on-plate trial welds were made with each consumable combination to optimize the welding parameters. Table 3 lists typical welding parameters for an average heat input of 2.2 kJ/mm (55 kJ/in.). A two-bead per layer welding technique was employed. Figure 1B shows a typical scheme of a completed narrow-groove weld, indicating the number of beads and the overlap configura-

Table 1—Chemical Composition of SA516-Gr. 70 Base Metal

Element (wt-%)						
C	Mn	P	S	Si	Al	Ni
0.21	0.11	0.013	0.012	0.385	0.030	0.105

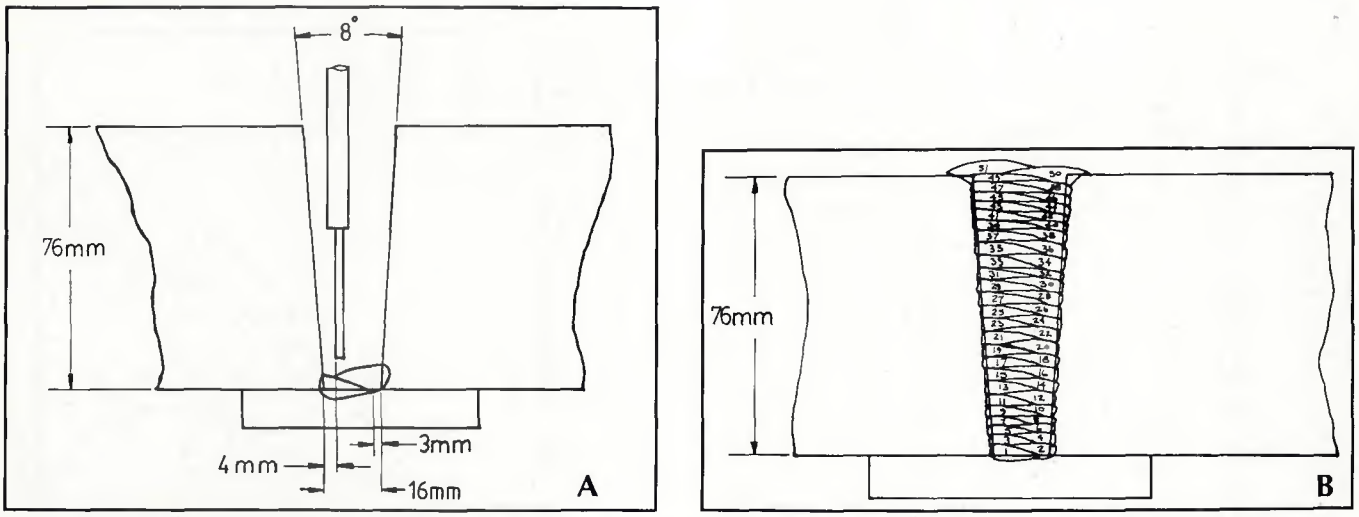

Fig. 1—A—Electrode position and bead location in narrow-groove welds; B—joint design and typical bead sequence of narrow-groove welds

tion. All welds were subjected to a post-weld heat treatment (PWHT) of 595°C (1103°F) for 2.5 h. Ultrasonic weld inspection was done in accordance with the ASME Section V standard.

Mechanical Testing and Metallography

All-weld-metal tensile and Charpy impact specimens were machined from the mid-thickness position of the test welds. The Charpy specimens were notched through-thickness at the ½-w (width) and ¼-w positions.

The percentage of as-deposited (columnar) and reheated weld metal regions were measured by optical microscopy at the ¼-w position. At the ½-w location, which is the overlap area between the two beads, there was approximately 80% reheated weld metal. The proportions of the microstructural constituents in the columnar region were determined by point counting in accordance with the current IIW classification scheme (Ref. 3).

The relative hardness of the as-deposited and reheated regions was determined using the Vickers method with a 500-g load.

Table 2—Welding Consumables

Weld No.	Wire (AWS)	Flux (Basicity)[a]	Principal Wire Alloy
NG-1	Oerlikon SD-3 (EM12K MOD)	Oerlikon OP121TT (3.0)	0.1 C 1.3–1.70 Mn
NG-2	Lincoln L-56 (EG)	Lincoln 880M (2.9)	0.1 C 1.20–1.85 Mn 0.8–1.15 Si
NG-3	Linde 40B (EA2)	Linde 80 (1.0)	0.1 C 0.45–1.35 Mn 0.45–0.65 Mo
NG-4	Linde 40B (EA2)	Linde 651VF (2.5)	0.1 C 0.95–1.35 Mn 0.45–0.65 Mo

(a) Basicity index (B.I.) was supplied by many factors and assumed to be based on the following formula:

$$B.I. = \frac{CaO + MgO + CaF_2 + \frac{1}{2}(MnO + FeO)}{SiO_2 + \frac{1}{2}(Al_2O_3 + TiO_2 + ZrO_2)}$$

Table 3—Welding Parameters for Narrow-Groove Welds

Current (AC square wave)	450–500 A
Wire feed speed	30 mm/s (71 ipm)
Voltage	32–34 V
Travel speed	7.4 mm/s (17.5 ipm)
Electrode extension	32 mm (1.25 in.)
Heat input	2.2 kJ/mm (55.9 kJ/in.)
Preheat (minimum)	93°C (200°F)
Interpass (maximum)	232°C (450°F)

Results

Chemical Composition

The chemical analyses and carbon equivalents of the weld metal deposits are provided in Table 4. In terms of hardenability, the carbon equivalent of Weld NG-2 was slightly higher than the other weld metals. In addition, the level of silicon is much higher in Weld NG-2.

The weld metal inclusion content can be directly related to the oxygen and sulfur levels. Note that Weld NG-3, made with an acid flux (B.I. = 1.0), had the highest oxygen content compared with the other three welds, which were deposited using more highly basic fluxes.

Tensile and Hardness Properties

The results of the all-weld-metal tensile tests of the four narrow-groove welds are given in Table 5. All welds met targeted yield (275 MPa) and ultimate tensile (482 MPa) strength levels, with Weld NG-2 having the highest strength.

The hardness results in Table 6 showed the same trend as the tensile strength results, with Weld NG-2 having the highest hardness in the as-deposited (columnar) region at the ¼-w position and at the ½-w location. Welds NG-3 and NG-4

Table 4—Chemical Composition of Narrow-Groove Welds

	Element[a] (wt-%)												
Weld	C	Mn	5i	P	S	Al	Ni	Cu	Cr	Mo	N	O	C.E.[b]
NG-1	0.11	1.37	0.35	0.013	0.008	0.013	0.05	0.19	0.025	<0.005	0.0099	0.018	0.36
NG-2	0.11	1.58	0.80	0.012	0.008	0.011	0.03	0.10	0.012	<0.005	0.0084	0.012	0.40
NG-3	0.07	0.91	0.52	0.012	0.017	0.006	0.03	0.15	0.015	0.49	0.0060	0.080	0.34
NG-4	0.07	1.08	0.11	0.015	0.010	0.008	0.02	0.15	0.020	0.47	0.0086	0.026	0.36

(a) Sn = 0.005% for all welds.

(b) $C.E. = C + \frac{Mn}{6} + \frac{Cr + Mo + V}{5} + \frac{Ni + Cu}{15}$

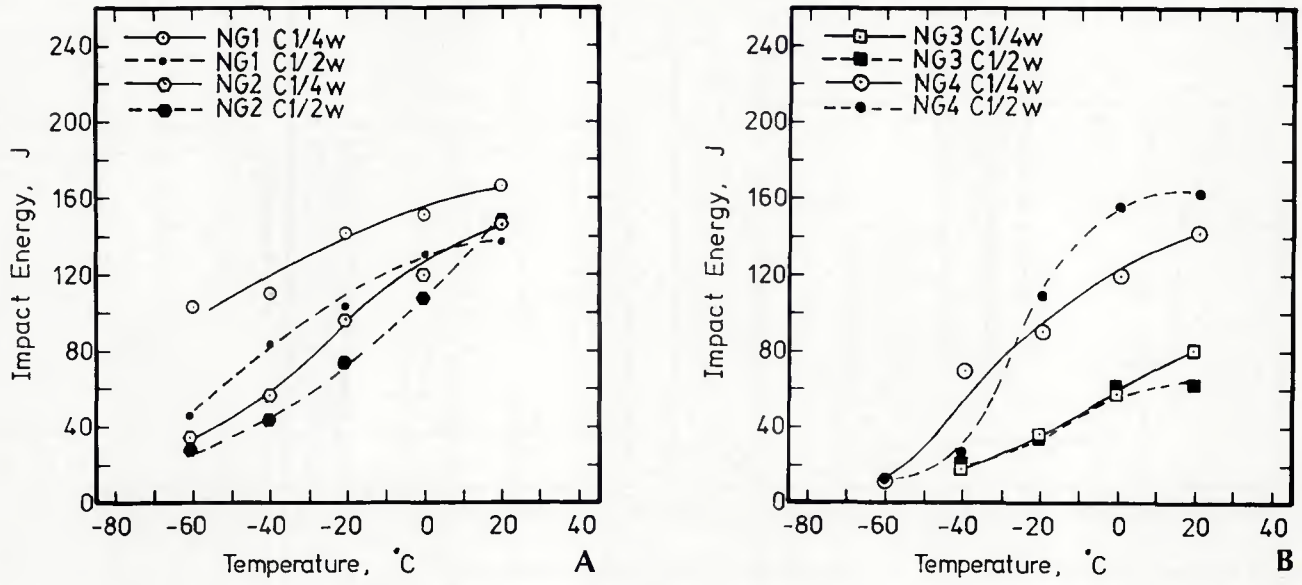

Fig. 2—Charpy impact transition curves of submerged arc narrow-groove welds; A—for NG-1 and NG-2; B—for NG-3 and NG-4

Table 5—Weld Tensile Properties

Weld No.	Yield Strength MPa (ksi)	Ultimate Strength MPa (ksi)	Elongation %	Reduction in Area %
NG-1	393 (57)	510 (74)	30	72
NG-2	446 (65)	575 (83)	30	70
NG-3	407 (59)	535 (78)	27	64
NG-4	421 (61)	519 (75)	33	71

Table 6—Microhardness of Narrow-Groove Weld Metals

Weld	Microhardness Vickers (500-g load) ¼ w Columnar	¼ w Reheated	½ w Reheated
NG-1	191	171	176
NG-2	207	176	197
NG-3	204	187	190
NG-4	203	195	186

had higher hardnesses than NG-1 and NG-2 in the reheated region at the ¼-w position.

Notch Toughness

Charpy transition curves generated for the four welds are shown in Fig. 2. In terms of the resistance to ductile fracture, Welds NG-1, NG-2 and NG-4 exhibited higher impact energies than Weld NG-3 for tests conducted at room temperature (20°C/68°F). This was irrespective of the location of notch position, which will be discussed later. Data points shown represent an average of at least three tests per temperature. The low-temperature brittle fracture resistance of the welds was evaluated by comparing the impact energies at −40°C. Weld NG-1 had the highest toughness overall. All welds, with the exception of NG-3 at ¼-w and ½-w positions and NG-4 at the ½-w position, met the targeted toughness levels of 27 J at −40°C.

The influence of the notch position on toughness was significant in Weld NG-1 and marginally significant in NG-2, with higher toughness exhibited at the ¼-w position. In Weld NG-4 the toughness was higher at the ½-w position for temperatures ≥−20°C (−4°F). There was no effect of notch position in Weld NG-3.

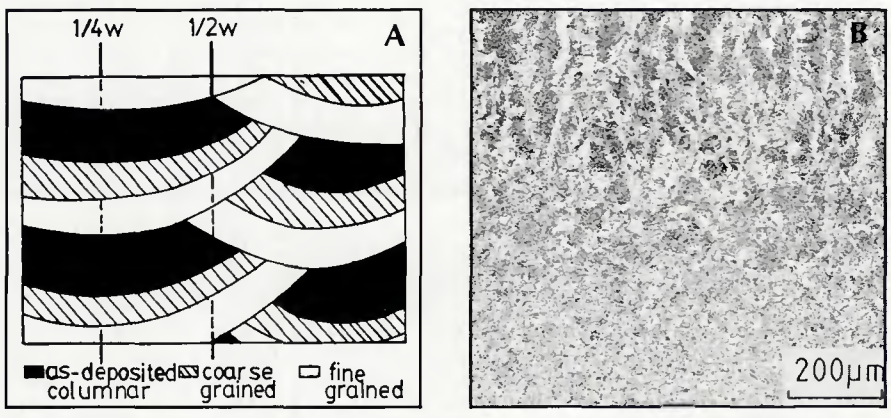

Fig. 3—Details of the weld metal microstructural regions. A—Schematic representation of weld metal regions in two pass per layer narrow-groove weld; B—structure of as-deposited (columnar), coarse- and fine-grained reheated weld metal regions at the ¼-w position

Microstructure

The microstructure for the narrow-groove welds, shown schematically in Fig. 3, consisted of as-deposited (columnar), coarse- and fine-grained reheated regions at the ¼-w position and primarily a reheated structure at the weld centerline (½-w position). All welds contained approximately 70% columnar and 30% reheated structure at the ¼-w position and 80% reheated structure at the ½-w position.

The as-deposited region of Welds NG-1 and NG-2, shown in Figs. 4A and 5A, consisted of an elongated columnar structure with grain boundary ferrite and ferrite with second phase at prior austenite grain boundaries. The second phase

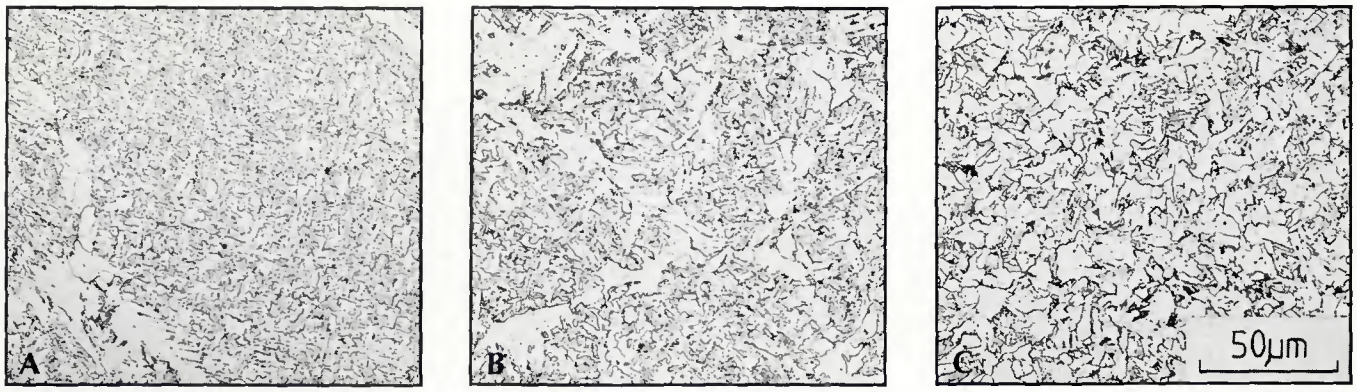

Fig. 4—Microstructures of Weld NG-1 after PWHT, nital etchant. A—As-deposited columnar region; B—coarse-grained reheated region; C—fine-grained reheated region

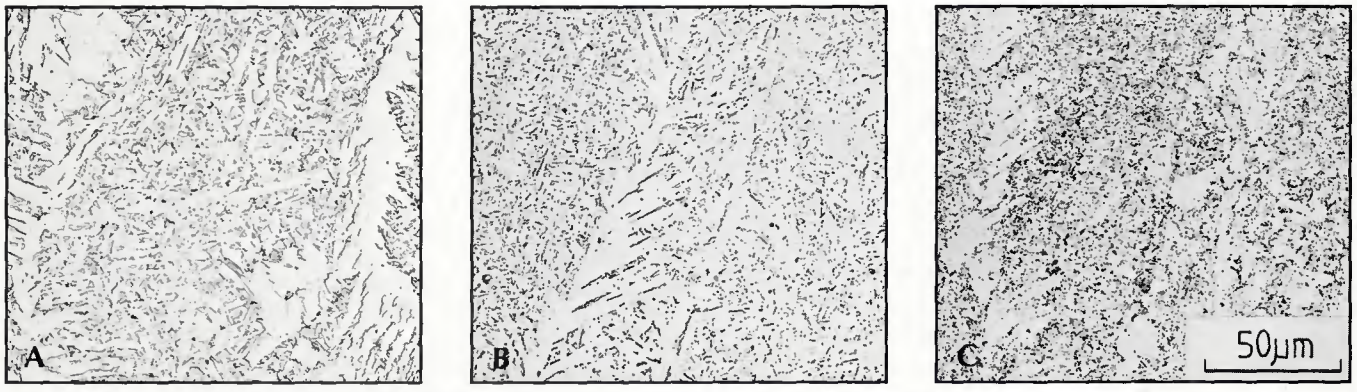

Fig. 5—As-deposited microstructure of Weld NG-2 in the as-welded and PWHT conditions. A—As-welded, nital etchant; B—as-welded showing M-A microphases, picral etchant; C—after PWHT showing carbide distribution, picral etchant

was composed of either elongated martensite-austenite (M-A) microphases or carbides. The M-A microphases were distinguished from carbides by using a picral etching solution. The M-A appears as a light etching constituent. Electron microscopy was used previously by the authors (Ref. 4) to identify that the M-A microphases contained retained austenite and twinned martensite.

The interior of the prior austenite grains was composed of acicular ferrite. The amounts of these microstructural constituents are listed in Table 7.

In the coarse-grained region, which constituted only 20% of the total reheated region, the reheating temperature exceeded the AC3 temperature producing an equiaxed microstructure with grain boundary ferrite at prior austenite grain boundaries and acicular ferrite within the grain interior—Fig. 4B. The fine-grained reheated region for Welds NG-1 and NG-2 features a polygonal ferrite structure interspersed with carbide aggregate, as shown in Fig. 4C. The fine-grained reheated structure was slightly coarser than the acicular ferrite in the as-deposited region. It should be noted that the PWHT, 595°C (1103°F)/2.5 h, did not alter the microstructural features of any of the welds, with the exception of the decomposition of martensite-austenite microphases in both columnar and reheated regions to form fine carbide particles along grain boundaries. The decomposition of microphases to form carbides is shown in Fig. 5.

The microstructures of Welds NG-3 and NG-4 at the ¼-w position are shown in Figs. 6 and 7. As recorded in Table 7 and illustrated in Fig. 6A, the columnar region of NG-3 featured coarse-grain boundary ferrite and ferrite with second phase. Weld NG-4 contained some grain boundary ferrite, but exhibited primarily a ferrite with aligned second phase in the columnar region, as shown in Fig. 7A. The high-volume fraction of spherical oxide inclusions (O + S = 0.097%) in Weld NG-3 as compared to the other welds is shown in Fig. 6A. The reheated region of NG-3 (Fig. 6B) contained a coarser polygonal ferrite than that found in NG-4—Fig. 7B.

Table 7—Proportions of Microstructural Constituents in the As-Deposited (Columnar) Weld Metal Region

	Percentage of Constituents				
			Ferrite with Second Phase		
Weld	Acicular Ferrite (AF)	Grain Boundary Ferrite (GF)	Aligned FS(A)	Nonaligned FS(N)	Polygonal Ferrite (PF)
NG-1	57	25	7	7	4
NG-2	59	22	7	8	4
NG-3	–	22	45	31	2
NG-4	–	15	75	7	3

Discussion

The results of the study have indicated that the mechanical properties (tensile strength and notch toughness) of thick-section, C-Mn narrow-groove welds can be achieved through appropriate selection of welding consumables. The control of notch toughness in particular, at temperatures representative of cleavage and ductile fracture, can be explained in terms of the interrelationship between weld chemistry and microstructure.

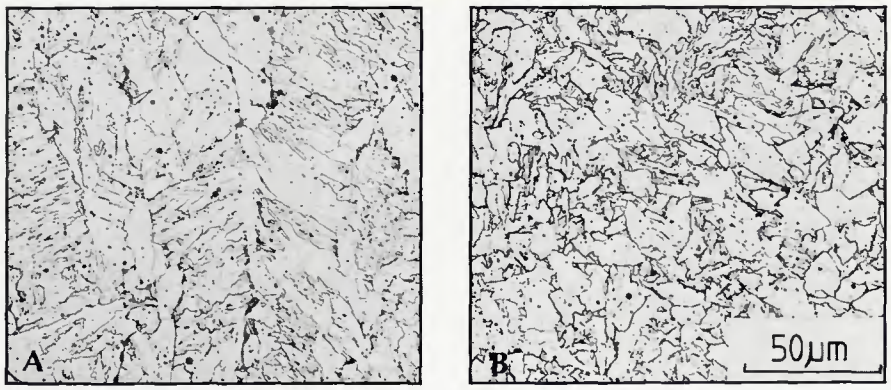

Fig. 6—Microstructures of Weld NG-3, after PWHT, nital etchant. A—As-deposited columnar; B—fine-grained reheated

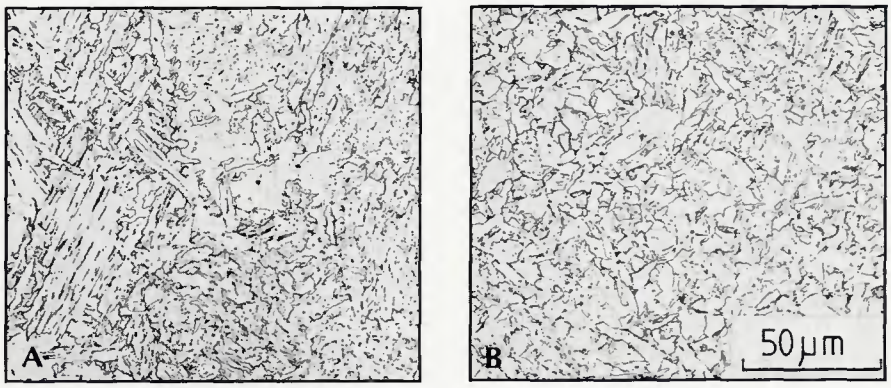

Fig. 7—Microstructures of Weld NG-4 after PWHT, nital etchant. A—As-deposited columnar; B—fine-grained reheated

Control of Weld Microstructure for Low-Temperature Fracture Resistance:

Welds NG-1 and NG-2

In Welds NG-1 and NG-2, the contribution of manganese is to lower the transformation temperature of austenite to ferrite (Ref. 5), thus increasing the proportion of acicular ferrite in the columnar region and refining the polygonal ferrite in the reheated region. The microstructural observations for NG-1 and NG-2 essentially agree with those of Evans (Ref. 6) who studied the effect of manganese content on the microstructure of shielded metal arc multipass welds. Evans found that a level of 1.4% Mn (C = 0.05%), resulting in approximately 65% acicular ferrite and fine polygonal ferrite in the columnar and reheated regions respectively, provided optimum notch toughness properties. In addition to the grain-refining effect of manganese in Welds NG-1 and NG-2, the role of weld metal inclusions as nucleation sites for the formation of acicular ferrite in the as-deposited region must be mentioned. It has been found (Ref. 7) that the formation of intragranular acicular ferrite was most prevalent in welds containing oxygen in the range of 200 to 450 ppm. However, in the present study, the fine inclusion particles in NG-1 and NG-2, resulting from a weld oxygen content in the range of 124 to 180 ppm, promoted acicular ferrite formation.

The shift of the Charpy transition curve to higher temperatures shown by Weld NG-2 compared with NG-1 (Fig. 2) can be attributed to the higher silicon level (0.8%) in Weld NG-2. A similar decrease in weld toughness with silicon addition has been documented (Refs. 8, 9). The work by Abson (Ref. 8) for submerged arc welds (SAW) and Evans (Ref. 9) for shielded metal arc welds (SMAW) have shown that increasing the silicon content up to 0.95% resulted in a slight increase in acicular ferrite and a significant increase in the formation of M-A microphases in the as-welded condition. Additionally, Evans showed that the microphases were replaced by carbide particles after PWHT. Thus, the increase in either M-A in the as-welded condition or carbide in the PWHT condition was considered to be responsible for the decrease in toughness with increasing silicon content. Although no quantitative assessment was made of the volume fraction of M-A microphases in the as-welded condition or carbides in the PWHT for Welds NG-1 and NG-2, their presence was verified particularly in Weld NG-2 (Fig. 5) by etching. It was assumed that the higher silicon level in NG-2 produced a greater amount of carbide particles in the PWHT condition, which resulted in the observed decrease in toughness at low temperatures.

Welds NG-3 and NG-4

The roles of inclusion content and molybdenum addition should be taken into account in analyzing the microstructure/low-temperature notch toughness property relationships in Welds NG-3 and NG-4. The coarse-grain boundary ferrite, and ferrite with second phase in the as-deposited region and the coarse polygonal ferrite in the reheated region of Weld NG-3 are promoted by the high-volume fraction of inclusion particles (O + S = 0.097%). Cochrane and Kirkwood (Ref. 10) proposed that in high oxygen-containing weld metals (oxygen $\geq$ 0.045%), the oxide inclusions provide pinning of austenite grain boundaries. The finer austenite grain size offered a larger grain boundary area for ferrite nucleation, and the transformation of austenite thus took place at a higher temperature. The sequence of events proposed by Cochrane and Kirkwood suggested that grain boundary ferrite nucleates initially followed by ferrite with aligned or nonaligned second phase.

The presence of ferrite with aligned second phase, observed partially in NG-3 and more prominently in NG-4, can be accounted for by the presence of the high (0.5%) level of Mo. The work of Ito and Nakanishi (Ref. 11) documented the effect of increasing Mo content on weld metal microstructure and notch toughness. They found that as the level of Mo was increased up to 0.3% an increase in acicular ferrite was observed in the weld metal, resulting in a significant increase in notch toughness. However, when the level of Mo was raised to 0.45%, a coarse lath structure was produced with a resultant sharp drop in toughness properties. Thus, the poor low-temperature ($T \leq -40°C$) toughness properties exhibited by both NG-3 and NG-4 weld metals can be accounted for by the presence of coarse-grain boundary ferrite and ferrite with aligned and nonaligned second phase in NG-3 and the ferrite with aligned second phase or lath structure observed in NG-4.

Control of Weld Microstructure for Resistance to Ductile Fracture

When impact testing is performed in the upper shelf region, the resistance to ductile fracture of weld metals is influenced by the volume fraction and size distribution of nonmetallic inclusions (Ref. 12). The inclusions are usually identified as oxysulfides. The mechanism for fracture is decohesion between inclusion particles and the matrix. Impact properties in the upper shelf region normally increase with decreasing oxygen and sulfur levels.

The current results indicate the same trend with Weld NG-3, which contains the highest O + S content and has the lowest shelf energy compared with Welds NG-1, NG-2 and NG-4, all with much lower O + S levels. The control of oxygen level in SAW welds comes principally from the selection of flux basicity.

Effect of Notch Position on Weld Toughness

In establishing the effect of notch position on the notch toughness in two-bead per layer multipass welds, the type of microstructure (as-deposited columnar and reheated regions) present at the root of the V-notch and their relative distributions must be taken into account. The existing data on the effect of notch position on weld notch toughness are conflicting (Refs. 13–15). Weld microstructure can vary significantly depending upon various factors such as composition, heat input, bead size and shape, and the precipitation of second phases; hence, there can be no general rule to explain the effect of notch position, and each weld must be analyzed individually.

For the present results, Welds NG-1 and NG-2 exhibited higher toughness when the notch was located in the center of the individual weld bead (¼-w position) compared to the center of the overlap location (½-w position). The improvement in toughness for NG-1 was significant and only marginal for Weld NG-2. The microstructure at the root of the notch for the ¼-w position contained 70% columnar and 30% reheated structure. The ½-w position featured approximately 80% reheated microstructure. One can account for the higher toughness if it is assumed that the mainly acicular ferrite structure in the columnar region at the ¼-w position provides superior resistance to fracture initiation and propagation than the fine polygonal ferrite in the mainly reheated structure at the ½-w position. Observations of fracture morphology in the ¼-w specimens confirmed that the fracture path propagated through acicular ferrite, as well as across the coarser grain boundary ferrite.

For Welds NG-3 and NG-4, the polygonal ferrite observed in the reheated structure at the ½-w notch position should provide superior resistance to brittle fracture as opposed to the coarse-grain boundary ferrite and ferrite with second phase observed in the columnar regions at the ¼-w position. However, no difference in toughness with notch position was observed for Weld NG-3, and the toughness data for NG-4 were not consistent (Fig. 2), *i.e.*, at low temperature, toughness was greater at the ¼-w position, while at elevated temperatures the opposite was true.

Optimization of Weld Chemistry

Based upon the weld microstructure observations and the resultant mechanical properties, the following weld chemistry is suggested in order to achieve the required weld metal strength and notch toughness properties: C ≈ 0.10%, Mn = 1.4–1.5%, Si = 0.25–0.35%, Mo ≤ 0.3%, O + S ≤ 0.030%.

The weld chemistry can be controlled by the selection of the welding wire and a basic flux.

Conclusions

The mechanical properties, *i.e.*, strength and notch toughness and the related microstructure, were evaluated for a series of welds deposited in thick-section SA516 Gr. 70 C-Mn steel using the submerged arc narrow-groove process. The following conclusions are listed:

1) All weld metals deposited with a range of wire chemistries (variations in Mn, Si, Mo contents) and flux basicities achieved the targeted tensile properties of 275-MPa (40-ksi) yield and 482-MPa (70-ksi) ultimate tensile strength.

2) Narrow-groove welds that achieved or exceeded the targeted notch toughness of 27 J (20 ft-lb) at −40°C (−40°F) contained a microstructure with a high proportion of acicular ferrite in the as-deposited columnar region and fine polygonal ferrite in the reheated region. The highest Charpy shelf energy was attained in welds containing a low-inclusion content, *i.e.*, O + S < 0.030%.

3) Welds that did not achieve the required low-temperature notch toughness properties contained a coarse-grain boundary ferrite and ferrite with second phase microstructure. The presence of a high-volume fraction of oxysulfide particles promoted the formation of grain boundary ferrite and ferrite with second phase. Additionally, the high level (0.5%) of molybdenum was considered responsible for the formation of ferrite with aligned second phase. It was also found that a high level of silicon, *i.e.*, 0.8%, can reduce low-temperature toughness by increasing the formation of M-A microphases, which transform to carbides during PWHT.

4) The effect of notch position on notch toughness was not conclusive. For the two-beads per layer configuration, significantly higher toughness was observed at the ¼-w notch position compared with the ½-w position for only one of the narrow-groove welds investigated.

Acknowledgment

The authors wish to thank D. E. Dolan and J. Newbury for their help in performing the experimental welding and nondestructive testing, respectively.

References

1. Chandel, R. S., Orr, R. F., Gianetto, J. A., McGrath, J. T., and Knight, R. F. 1985. The mechanical properties of 2.25Cr-1Mo weld metals deposited by the SAW-NG process. *J. of Mat. for Energy Systems* 7(2):137–146.

2. Chandel, R. S., Orr, R. F., Gianetto, J. A., McGrath, J. T., Patchett, B. M., and Bricknell, A. C. 1985. The microstructure and mechanical properties of narrow gap welds in 2.25 Cr-1Mo steel. *Int. Inst. of Welding Doc. IX-1355-85.*

3. Pargeter, R. J., and Dolby, R. E. 1985. Guidelines for classification of ferritic steel weld metal microstructural constituents using the light microscope. *Int. Inst. of Welding Doc. IX-1377-85.*

4. Glover, A. G., McGrath, J. T., Tinkler, M. J., and Weatherly, G. C. 1977. The influence of cooling rate and composition on weld metal microstructures in C/Mn and a HSLA steel. *Welding Journal* 56(9):267-s to 273-s.

5. Paxton, H. W. 1981. The metallurgy of steels for large diameter linepipe. *Alloys for the Eighties,* pp. 185–211. Climax Molybdenum Co.

6. Evans, G. M. 1983. Effect of manganese on the microstructure and properties of all-weld-metal deposits. *Welding Research Abroad* 29(1):2–12.

7. Abson, D. J., Dolby, R. E., Hart, P. H. M. 1978. The role of nonmetallic inclusions in ferrite nucleation in carbon steel weld metals. *Trends in Steels and Consumables for Welding* 25:75–100, The Welding Institute.

8. Abson, D. J. 1978. *A Study of the Influence of C and Si on the Microstructure and Toughness of Submerged Arc Welds.* Welding Institute Members Report. 68/1978/M.

9. Evans, G. M. 1986. Effect of silicon on the microstructure and properties of C-Mn all-weld-metal deposits. *Metal Construction* 18(7):438R–444R.

10. Cochrane, R. C., and Kirkwood, R. P. 1978. The effect of oxygen on weld metal microstructure. *Trends in Steel and Consumables for Welding* 35:103–121. The Welding Institute.

11. Ito, Y., and Nakanishi, M. 1976. Study on Charpy impact properties of weld metal with submerged arc welding. *The Sumitomo Search* May(15):42–62.

12. Taylor, L. G., and Farrar, R. A. 1975. Metallurgical aspects of the mechanical properties of the submerged arc weld metal. *Welding and Metal Fabrication* 43(4):305–310.

13. Dittrich, S., and Grosse-Wordemann, J. 1985. 2.25 Cr-1Mo filler metals with high toughness properties after step cooling. *Proc. of Int. Conf. on Welding for Challenging Environments,* pp. 273–281.

14. Nakanishi, M., Katsumoto, N., Kawai, K., and Tsumura, H. 1986. Development of high strength welding materials for low temperature service. *The Sumitomo Search* May (32):97–105.

15. Tweed, J. H., and Knott, J. F. 1983. Effect of reheating on microstructure and toughness of C-Mn weld metal. *Metal Science* 17(Feb.):45–54.